AD-A066 494 NAVAL POSTGRADUATE SCHOOL MONTEREY CALIF F/G 21/8
AN EXPERIMENTAL INVESTIGATION OF THE DUAL CHAMBER ROCKET,(U)
JAN 79 J F MCFILLIN, D W NETZER

UNCLASSIFIED NPS67-79-001 NL

| OF |
AD
A066494

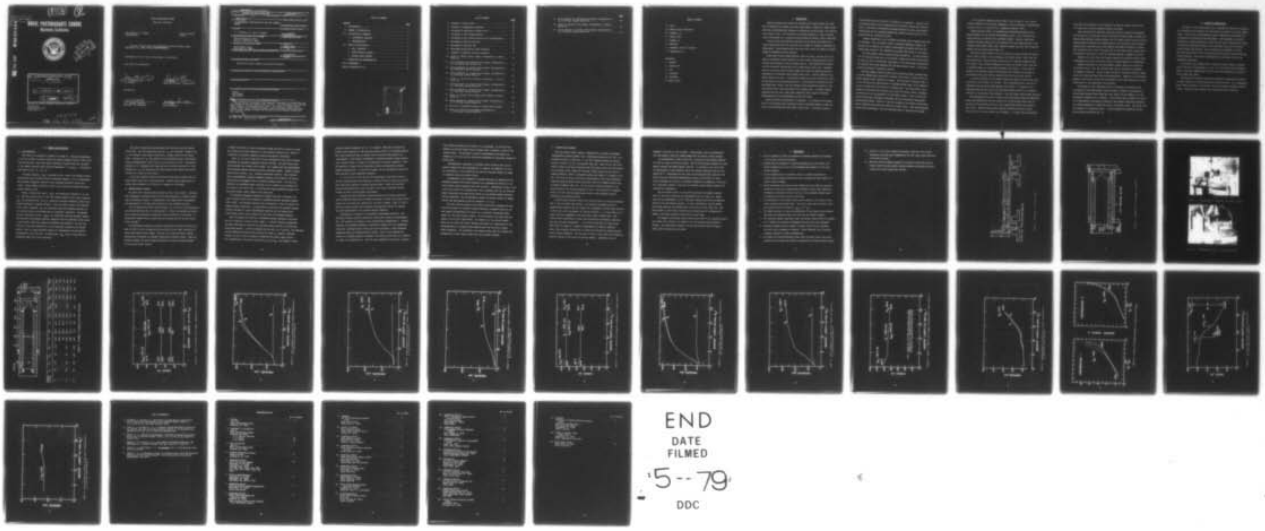

END
DATE
FILMED
5-79
DDC

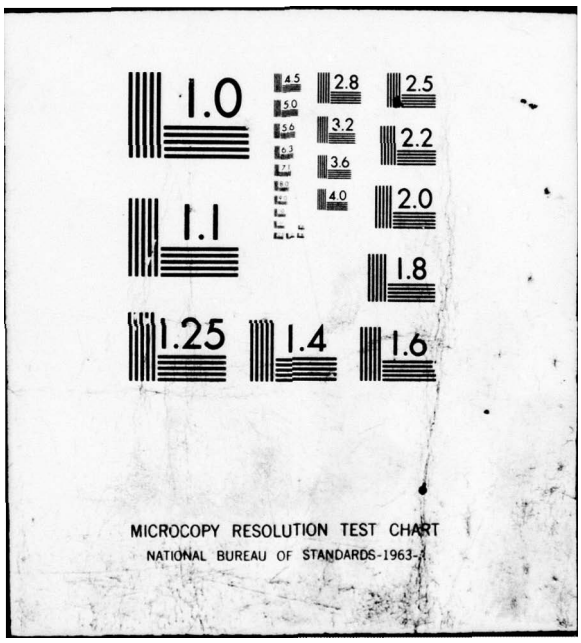
1.0
1.1
1.25
1.4
1.6
1.8
2.0
2.2
2.5
2.8
3.2
3.6
4.0
4.5
5.0
5.6
6.3
MICROCOPY RESOLUTION TEST CHART
NATIONAL BUREAU OF STANDARDS-1963-A

(14) NPS67-79-001

NAVAL POSTGRADUATE SCHOOL

Monterey, California

(6) AN EXPERIMENTAL INVESTIGATION OF THE DUAL CHAMBER ROCKET

(10) J. F./McFillin, Jr. [redacted] D. W./Netzer

(11) Jan[redacted]79 (12) 48 p.

Prepared for:
Naval Weapons Center
China Lake, CA

NAVAL POSTGRADUATE SCHOOL

Monterey, California

Rear Admiral T. F. Dedman
Superintendent

Jack R. Borsting
Provost

The work reported herein was supported by the Naval Weapons Center, China Lake, CA., under contract N6053078WR30023.

This report was prepared by:

J. F. MC FILLIN, JR.
LT, US NAVY

D. W. NETZER
Associate Professor of Aeronautics

Reviewed by:

M. F. PLATZER, Chairman
Department of Aeronautics

W. M. TOLLES
Dean of Research

UNCLASSIFIED
SECURITY CLASSIFICATION OF THIS PAGE (When Data Entered)

REPORT DOCUMENTATION PAGE		READ INSTRUCTIONS BEFORE COMPLETING FORM
1. REPORT NUMBER NPS67-79-001	2. GOVT ACCESSION NO.	3. RECIPIENT'S CATALOG NUMBER
4. TITLE (and Subtitle) AN EXPERIMENTAL INVESTIGATION OF THE DUAL CHAMBER ROCKET		5. TYPE OF REPORT & PERIOD COVERED 6. PERFORMING ORG. REPORT NUMBER
7. AUTHOR(s) J. F. McFillin, Jr. and D. W. Netzer		8. CONTRACT OR GRANT NUMBER(s) N6053078WR30023
9. PERFORMING ORGANIZATION NAME AND ADDRESS Naval Postgraduate School Monterey, California 93940		10. PROGRAM ELEMENT, PROJECT, TASK AREA & WORK UNIT NUMBERS
11. CONTROLLING OFFICE NAME AND ADDRESS Naval Weapons Center China Lake, CA 93555		12. REPORT DATE January 1979 13. NUMBER OF PAGES 46
14. MONITORING AGENCY NAME & ADDRESS(if different from Controlling Office)		15. SECURITY CLASS. (of this report) Unclassified 15a. DECLASSIFICATION/DOWNGRADING SCHEDULE

16. DISTRIBUTION STATEMENT (of this Report)

Approved for public release; distribution unlimited.

17. DISTRIBUTION STATEMENT (of the abstract entered in Block 20, if different from Report)

18. SUPPLEMENTARY NOTES

19. KEY WORDS (Continue on reverse side if necessary and identify by block number)

Rocket
Dual Chamber
Experimental

20. ABSTRACT (Continue on reverse side if necessary and identify by block number)

An experimental investigation was conducted to determine the feasibility and practicality of the dual chamber rocket concept. Cold flow studies were performed which utilized a telescoping booster cavity. The effects of booster cavity length, booster cavity shockdown pressure, booster/sustainer nozzle area ratio, and aft nozzle removal on thrust and the booster cavity pressure distribution were explored.

DD FORM 1 JAN 73 1473 EDITION OF 1 NOV 65 IS OBSOLETE
S/N 0102-014-6601

UNCLASSIFIED
SECURITY CLASSIFICATION OF THIS PAGE (When Data Entered)

TABLE OF CONTENTS

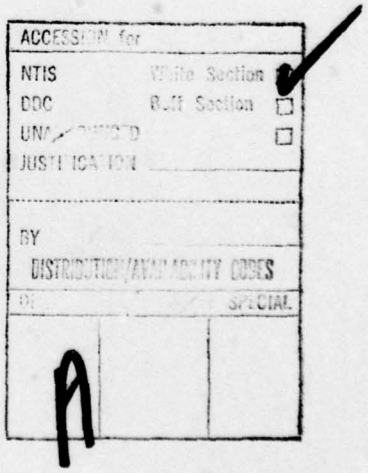

LIST OF FIGURES

TABLE OF SYMBOLS

A = Area

C_f = Nozzle thrust coefficient

d = Diameter, in.

F = Thrust, lbf.

L = Length, in.

$\dot{m}$ = Flowrate

P = Pressure, lbf./in.^{2} absolute

T = Temperature, °R

Subscripts:

b = Booster

e = Nozzle exit

j = Jet

s = Sustainer

sh = Shockdown

t = Nozzle throat

I. INTRODUCTION

Tactical missiles most often have utilized solid fueled rockets for their ease of handling and storage, and their light weight. Demands for higher performance have necessitated new advances in propellants and metallurgy, and pressures have steadily risen. New inovations have become necessary in order to improve overall performance for a propulsion system which has become a mature technology.

Various thrust-time behaviors obtained with new grain configuration and nozzle combinations have been utilized in an attempt to optimize performance for design goals. Boost-sustain motors have been used to meet the demand for medium ranged air-launched tactical missiles.

Boost motors utilize high pressures, high burn rates, and thus short burn times to accelerate tactical missiles to their normal operating speeds, and to provide rapid separation from the launch vehicle. This generally has necessitated an internally burning grain and a large nozzle throat area. Sustainer motors, on the other hand, require longer burn times and operating pressures determined by the desired boost-sustain thrust ratio. Current demands are for thrust ratios up to 20:1. A particular problem occurs when large thrust ratios are required for the boost-sustain motor. If both modes of operation use the same large boost nozzle, then the sustainer would necessarily operate at very low pressures with often unacceptably low burning rates. To obtain adequate pressures and flow rates under these conditions often requires internally burning grains with correspondingly shorter burn times.

Several possible alternatives are available. In principle, the burning rate of the sustainer motor propellant could be increased enough to allow the use of an end burning grain with small surface area. In practice, however,

high burning rates are difficult to obtain at low pressures. Separate boost and sustain motors could be employed with the booster ejected after burnout. This is often done on ground/ship launched missiles, but this would present difficulties for air launched systems which usually utilize one set of aft mounted fins for trajectory control.

Another alternative is the variable area nozzle, which requires some form of actuation. This, by itself, leads to increased complexity, weight, and expense, not to mention the technical difficulties associated with the high temperatures involved. New technology may permit this concept in the future.

The dual-chamber rocket presents another alternative. In this configuration the sustainer motor has its own nozzle, raising the pressure sufficiently to allow the use of conventional propellants in the end-burning configuration. The sustainer motor then exhausts into the empty booster cavity. The booster nozzle may either be retained or ejected.

The dual chamber concept involves some interesting design considerations. A typical design might incorporate a booster cavity which is nearly fifty sustainer exhaust nozzle diameters in length. From available literature [Refs. 1, 2, 3], free jets have been observed to shockdown within eight to ten diameters. Little is known about the behavior of confined jets. For long booster cavity lengths the sustainer motor exhaust would enter the booster cavity, shockdown, and merely act as a gas generator for the booster nozzle. This in itself may provide sufficient performance advantages over the conventional (one-nozzle) boost-sustain design. However, if the jet impinges on the booster cavity walls, severe problems could arise from high heat transfer rates. This could adversely affect thrust performance, with the increased need for insulation and weight.

If the sustainer exhaust could be made to pass through the boost cavity without shockdown or only partial shockdown, it may be possible to significantly increase thrust as a result of lower stagnation pressure losses.

Benham and Wirtz [Ref. 4] concluded that preventing shockdown did not appear feasible for the tactical dual-chamber concept. This conclusion was based primarily on observed short shockdown lengths. However, these short shockdown distances might still prove beneficial in the tandem approach to the integral-rocket-ramjet (IRR), where combustor lengths are short and the booster exhaust jet may actually pump ramjet air.

The above concept requires that the sustainer jet pass through the booster nozzle, either freely or just attaching at the nozzle throat. While this may not be practical, another possible means exists for reducing stagnation pressure losses. This involves designing the nozzles and booster cavity such that it operates similar to a blow-down supersonic wind tunnel. In this mode of operation the sustainer exhaust would expand (with minimum or no shocks) to the booster cavity wall and flow supersonically into the booster nozzle.

In order to operate in this manner, particular values of nozzle area ratio, and booster cavity length are required. These requirements may or may not be compatible with particular motor geometry restrictions. To operate in the supersonic mode may also require the sustainer exhaust nozzle to be specially contoured to the booster cavity diameter. This may impose severe weight penalties.

The approximate area ratios required can be determined using one-dimensional theory and assuming that the only losses occur across normal shocks (Ref. 5). The value of the specific heat ratio will significantly affect the required area ratios. Smaller values require smaller sustainer and booster nozzle throat areas for a given booster cavity diameter. It should also be mentioned

that both the "starting" of the supersonic flow and the exhaust nozzle losses will depend upon the local ambient pressure (altitude).

When calculating the necessary area ratios several operating requirements must be met; (a) the sustainer nozzle throat must be small enough to produce the desired high sustainer chamber pressure, (2) the booster throat area must provide adequate booster pressure and loading fraction, (3) the booster throat pressure during sustain operation must be kept greater than ambient pressure to prevent flow separation and to allow "starting" and (4) the booster cavity length probably should be sufficient to allow the sustainer exhaust to expand to the wall.

Whether or not the above restrictions together with possible nozzle contour requirements will allow a practical system to operate remains to be determined.

Another alternative for the dual-chamber concept employs the ejection of the booster nozzle. Here the sustainer motor may be optimized for expansion to atmospheric pressure. Thrust is again provided at sustainer pressures commensurate with long burn times using end burning grains. Expansion of the sustainer exhaust to the booster cavity wall could greatly affect base pressure and thereby cause thrust to vary appreciably with altitude.

The purpose of this investigation was to determine the feasibility and practicality of the dual-chamber concept through a systematic investigation of the pertinent design (nozzle shape and size, booster cavity lengths, etc.) and operational (pressure, etc.) variables. This initial report presents the results of an experimental investigation directed at dual-chamber operating characteristics without expansion to supersonic flow in the booster cavity. The latter will be presented in a subsequent report. Initial mathematical modelling work has been previously published (Ref. 6).

II. METHOD OF INVESTIGATION

The object of this investigation was to determine the effects of configuration variables on the internal flow field and on the thrust of the dual chamber rocket. To this end, both axisymmetric and 2-D apparatus were designed and constructed for non-reacting flow experiments. The axisymmetric apparatus consisted of a telescoping booster cavity and was used to determine the effects of design and operating variables on the obtainable thrust and the booster cavity pressure distribution. The 2-D apparatus was designed to provide schlieren observations of the flow field within the booster cavity during sustainer operation. This initial investigation was concerned only with the axisymmetric apparatus.

The booster cavity length could be varied to provide length to diameter ratios from zero to approximately 2.3 for a 4.0 inch booster cavity diameter. Thrust, pressures, temperatures, and flow rates were measured and recorded as cavity length was varied.

Two booster and sustainer nozzles were employed to determine the effects of nozzle diameter, and booster/sustainer nozzle area ratio. As a consequence, nozzle exhaust pressure to the booster cavity and shockdown pressure could be varied. Sustainer motor pressures were varied from 1500 to 300 psia.

III. DESCRIPTION OF APPARATUS

A. AXISYMMETRIC APPARATUS

The axisymmetric motor was mounted on a thrust stand which utilized linear bearings to minimize frictional effects (Fig. 1). Figure 2 presents a schematic of the dual chamber apparatus. The high pressure section was mounted to the thrust stand. The length of the low pressure section could be varied by actuation of a hydraulic jack mounted on the aft end of the thrust stand. This section was also mounted on linear bearings. Photographs of the apparatus are presented in Figures 3 through 8. Figures 4 and 5 show the apparatus in the full forward position and Figure 6 in the full aft position.

To ensure that no forces from the high pressure air supply interacted with the thrust developed by the nozzle, two flexible hoses twenty feet in length were utilized (Fig. 8).

The air supply system consisted of a small 3500 psi air compressor, air dryer, and storage tanks.

Three basic configurations were employed in the initial investigation as summarized in Figure 9.

B. INSTRUMENTATION

Thrust was measured with a strain gage load cell and calibrated using a pulley and weight-table arrangement. Air flow rate could be measured using an A.S.M.E. sharp edged orifice. Orifice pressure and differential pressure and sustainer cavity pressure transducers were calibrated using a dead-weight tester. Booster cavity length was measured using a linear potentiometer attached to the translating section. Pressure distribution within the booster cavity was measured using a Statham differential pressure transducer mounted in a 48-channel Scanivalve.

Scanivalve output, orifice temperature, and booster cavity temperature were recorded on strip-chart recorders. All other variables were recorded on an 8-inch Visicorder.

IV. RESULTS AND DISCUSSION

A. DATA REDUCTION

The results are presented in Figures 10 through 23. During the experiments it was not possible to exactly obtain the desired pressure levels of 1500, 1000, 500, and 300 psia. When these small variations occurred thrust was corrected to the nominal pressure value using the expression $F = C_F P_T A_t$. Corrections were made for both P_T and C_F.

Shockdown pressures (P_{sh}) presented in Fig. 9 and on the pressure distribution plots were calculated from the continuity equation (i.e. by multiplying the sustainer stagnation pressure by the sustainer-to-booster throat area ratio). Nozzle exhaust pressures in Fig. 9 were calculated assuming one-dimensional isentropic flow.

Values of theoretical thrust (F_{th}) are presented in Figures 10, 14, and 17. With the booster cavity in the full forward position (left side of figures) F_{TH} was calculated from $C_F P_T A_t$ using the sustainer stagnation pressure and nozzle exhausting to ambient pressure. With the booster cavity fully extended (right side of figures) F_{TH} was calculated using the shockdown pressure for P_T and the booster nozzle exhausting to atmospheric conditions. The maximum possible theoretical thrust (F_{max}) was calculated using the sustainer stagnation pressure and assuming isentropic expansion from the sustainer nozzle throat to the booster nozzle exit diameter and ambient back pressure. For this calculation it was also assumed that no flow separation occurred in the booster noozle. This is a good assumption except for configuration (3) and possibly configuration (1) at 500 psia. In these cases F_{max} may be larger than the calculated value due to flow separation.

Only minor variations occurred between the pressures along the booster cavity wall. For this reason only data for p_6 are presented. Pressure tap p_6 was located in the booster cavity wall, 2 inches forward of the nozzle plate. Pressure tap p_9 was located in the diverging section of the booster nozzle (configurations 1 and 2 only) at an area ratio of 1.237. This nozzle employed a 5.5° divergence half angle and had an overall area ratio of 1.362. Pressure tap p_8 was located on the booster nozzle plate (above the contour section) at a radius of 0.90 inches.

In the full forward position the booster nozzle did not contact the sustainer nozzle plate (due to bearing stops). Booster cavity length could be varied from a minimum of 0.35 inches to a maximum of 9.28 inches.

B. BOOSTER NOZZLE ATTACHED

The three basic configurations presented in Fig. 9 were tested. Configuration 1 employed a sustainer nozzle that provided expansion to slightly greater than the shockdown pressure. Configuration 2 was significantly overexpanded and configuration 3 provided ideal expansion to the shockdown pressure.

Fig. 10 presents the thrust data and Figs. 11, 12, and 13 the corresponding pressure distribution data for configuration 1. Thrust was measured as booster cavity length was decreased continuously from 9.28 inches to 0.35 inches. At intermittent lengths booster length was held constant and the pressure distribution recorded.

The differences between the sustainer and booster theoretical thrusts was small (3-13%) for this configuration and resulted in very minor variations in thrust with booster cavity length. However, at no time did thrust increase dramatically to approach the maximum theoretically possible thrust. Thus, the sustainer exhaust jet never remained supersonic and never smoothly attached to the booster nozzle contour.

It might be possible to tailor the booster length and nozzle contours to permit the latter but it would probably be a very unstable condition (as a result of variations in sustainer stagnation pressure and ambient conditions).

Figs. 11, 12, and 13 show that for this configuration wall static pressure approached the shockdown stagnation pressure (85-93%). The wall static pressure decreased with booster cavity length. For lengths less than approximately 18-20 sustainer exhaust diameters pressure decreased rapidly. However, booster nozzle static pressure (p_9) remained essentially constant. This indicated that an approximately constant stagnation pressure was provided to the booster nozzle and is in agreement with the observed constant thrust. For this configuration jet shockdown always occurred, but the subsonic jet apparently did not spread to the cavity wall. A recirculation region apparently existed over the entire booster cavity length at the outer wall.

As sustainer stagnation pressure was reduced from 1500 to 500 psia, the ratio of booster wall static pressure to shockdown pressure decreased slightly (93% to 85%). The pressure profiles also are observed to level off earlier for higher pressure conditions. It should also be noted that the sustainer exhaust actually operated in a more underexpanded condition than the design point since booster cavity static pressure was less than the shockdown pressure.

Fig. 19 presents the fraction of shockdown pressure obtained at the outer wall as a function of booster cavity length. If several plausible assumptions are made (which must be verified with schlieren data) then Fig. 19 yields some interesting results. It will be assumed that (a) when p_6 (or p_8) $\approx P_{sh}$ the expanding jet has reached the booster cavity wall and (b) when p_6 begins to decrease rapidly, the core of the jet begins to penetrate the booster nozzle throat (for configuration 1 the latter occurred for $p_6 \approx 0.7P_{sh}$ and lengths of 16-20

sustainer exhaust diameters, or 4.4 - 5.5 inches). When the jet clears the booster nozzle entirely it will pump the booster cavity to its minimum pressure. With these assumptions Fig. 19 implies that the jet may have spread in an approximately linear manner independent of sustainer pressure (since pressure ratio remained fixed) to lengths of approximately 18 exhaust diameters. After 18 diameters of length the jet spread more slowly and approached a maximum diameter asymtotically. In the latter stages, the jet spreading was slower for lower sustainer nozzle stagnation pressures.

It is not clear at this time why the percentage of theoretical thrust at 500 psia increased above that obtained at 1000 psia and why values were greater than theoretical possible at maximum booster length. Thrust and sustainer pressure measurements were least accurate at low thrust conditions and may account for some of this apparent discrepancy.

Although the small difference between sustainer and booster theoretical thrust prohibited observation of marked variations in thrust with booster cavity length some variations were observed for very short lengths. Figs. 11, and 12 show that booster nozzle static pressure decreased more rapidly for lengths less than approximately five sustainer exhaust diameters.

Configuration 2 operated in an extremely overexpanded condition. The difference between sustainer and booster theoretical thrusts was approximately 13%. The behavior was similar to that obtained with configuration 1. However, sustainer jet shockdown apparently occurred more rapidly for the overexpanded conditions, allowing booster cavity wall static pressures to reach shockdown stagnation values for maximum booster lengths. Fig. 19 also presents the fraction of shockdown pressure attained at the booster cavity wall as a function of length for configuration 2. With the same assumptions used above it appears

that sustainer pressure had no affect on jet spreading. In this case the exhaust jet was much larger and more nearly equal in diameter to that of the booster throat. 70% shockdown occurred at approximately six exhaust jet diameters (or 2.8 in) and the subsonically expanding jet apparently reached the booster wall.

Configuration 2 exhibited a noticeable thrust increase (Fig. 14) for booster lengths less than approximately 3.5 exhaust jet diameters (1.6 in.). For configuration 2 this apparently was when the sustainer exhaust jet began to completely clear the booster throat.

Configuration 3 was designed for optimum sustainer jet expansion to the shockdown pressure but actually operated in an underexpanded mode due to the lower booster cavity pressures which were obtained. Comparisons of Figs. 17 and 18 with the results for configurations 1 and 2 indicates that the jet core had begun to penetrate the large booster nozzle at the maximum lengths obtainable with the apparatus. The jet apparently cleared the booster nozzle for lengths shorter than approximately seven jet diameters (3.3 in.).

The above results indicate that without specifically designing the area ratios and lengths (to simulate blowdown supersonic windtunnel behavior) the dual chamber configuration will operate in a completely shockdowned manner except for very short booster lengths. Thrust variation with length does not appear to be of major significance. The behavior for the shorter lengths where the jet clears the booster exhaust nozzle may be of significance in the design/operation of integral-rocket-ramjets which use very short coupled ramjet combustors. Jet spreading to the booster cavity wall (as occurred with configuration 2) may present significant heat transfer problems.

C. BOOSTER NOZZLE REMOVED

With the booster nozzle removed, configuration 1 provided an extremely underexpanded sustainer exhaust flow. Theoretical thrust was 90.7 lbf. for a sustainer pressure of 1500 psia. In the full forward position (no booster cavity) a thrust of 81 lbf. was measured (Fig. 20). Thus, 10 lbf. was attributed to drag on the thrust apparatus when the booster cavity was full-forward. As the booster cavity length was increased, thrust dropped slowly until 18 exhaust diameters, where it decreased rapidly with length to a minimum of 28.6 lbf. This drop in thrust was directly attributable to less than atmospheric pressures being developed within the booster cavity for lengths greater than 12 exhaust diameters (Fig. 21). At the full aft position pressure on the forward booster wall was approximately 10 psia. This resulted in a negative thrust of 61 lbf. and was approximately equal to the difference between theoretical and measured thrusts.

A large thrust variation would occur from sea level to forty-five thousand feet if the aft nozzle were ejected. The altitude performance would be significantly improved over the "nozzle on" performance, but this wide variation in thrust may not be acceptable for tactical missiles. It is well known in air combat that most engagements take place below twenty thousand feet. Most pilots would be unwilling to accept such inconsistent performance, especially such poor sea level performance. It is worth noting that the rapid thrust decay (Fig. 20) began at a length of approximately 18 exhaust diameters. Large, high frequency oscillations in thrust also occurred for lengths greater than 18 exhaust diameters. The top curve in Fig. 21 also shows that atmospheric pressure existed in the cavity for shorter lengths. Apparently, the jet

expanded to the wall at this location. Interestingly, this was approximately the same length at which jet pumping began with the booster nozzle attached.

In configuration 2 (Figs. 22 and 23), a sustainer nozzle exhaust diameter of 0.465 in. (vice 0.273) was utilized. The jet had increased diameter but lower exhaust pressure and higher exhaust velocity. It attached to the cavity wall at approximately 13 exit diameters (about 20% further downstream than for configuration 1). Decreasing the flow rate (by reducing sustainer pressures from 1500 to 300 psia) decreased underexpansion effects and resulted in a more slowly spreading jet (from 13 to 18 exhaust diameters for expansion to the wall). For a sustainer pressure of 300 psia the sustainer nozzle exhaust pressure was approximately atmospheric.

For the booster cavity in the full-aft position the negative pressure thrust at sea level conditions was approximately 40 lbf. (Fig. 22). Again, there was an approximately 10 lbf. difference between theoretical and measured thrust in the full-forward position. In this configuration the jet expands more slowly and does less pumping down of the booster cavity (Fig. 23). This would result in less thrust variation with altitude than for configuration 1. However, the thrust variation would still be quite large.

The length of the booster cavity and the area ratio of the sustainer nozzle will affect the decision as to whether or not the booster nozzle should be ejected. For long booster cavities, aft end heat transfer would be high as would thrust variation with altitude.

V. CONCLUSIONS

1. For the geometries tested, no evidence of sustainer exhaust jet attachment to the booster nozzle was obtained.
2. Without specific attention to nozzle contouring and to area ratios, sustainer operation will occur in the shockdown mode (except for very short booster lengths).
3. In the shockdown mode of operation, thrust is usually insensitive to booster length although booster wall static pressure may drop rapidly with shorter booster lengths.
4. Thrust variations with booster cavity length will occur when the sustainer and booster nozzles have significantly different thrusts (when expanded to atmospheric conditions) and when the core of the sustainer exhaust begins to penetrate the booster nozzle throat area.
5. Jet penetration of the booster nozzle throat results in the booster cavity static pressure being pumped down. The drop in wall static pressure occurs more rapidly below the condition $p_{wall} = 0.7\ P_{sh}$.
6. The length required to obtain jet penetration of the booster nozzle depends upon both the sustainer nozzle area ratio and the exhaust diameter.
7. The sustainer exhaust completely clears the booster nozzle throat for lengths of 3-7 exhaust jet diameters (depending upon the nozzle areas employed).
8. Sustainer pressure does not appear to greatly affect the jet spreading rate until after shockdown is complete. After shockdown, lower sustainer pressures resulted in slower spreading rate.
9. The higher the booster/sustainer thrust ratio the lower will be the static pressure on the booster wall (more jet penetration of booster nozzle throat).

10. **Ejection of the booster nozzle for sustainer operation could provide significant altitude thrust augmentation but also rapid thrust reduction as altitude decreased.**

11. **When the sustainer exhaust spreads to the booster cavity wall and the booster nozzle has been removed, system vibration and booster wall heat transfer may become significant problems.**

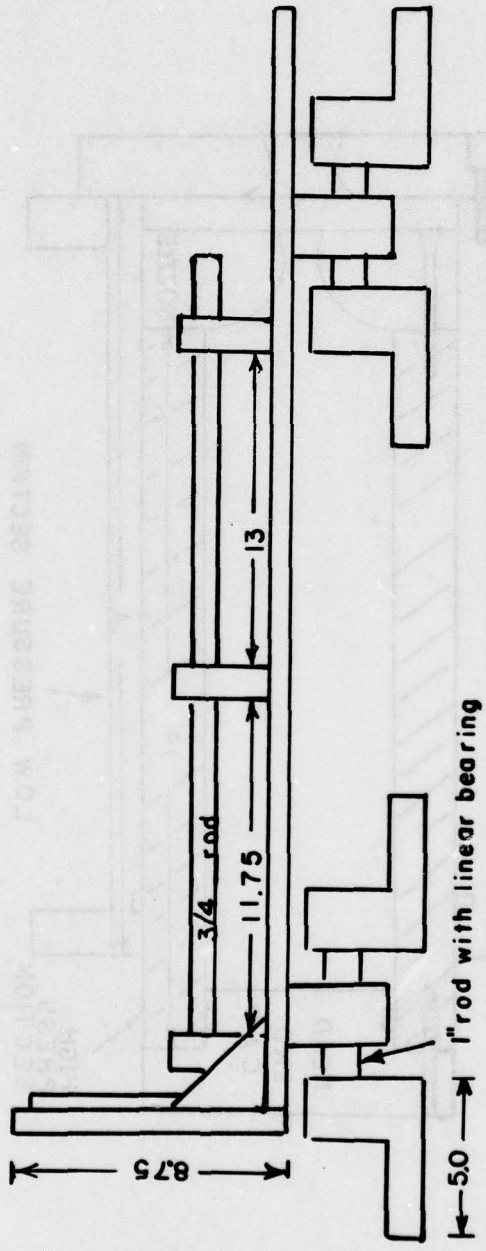

Figure 1. Schematic of Thrust Stand.

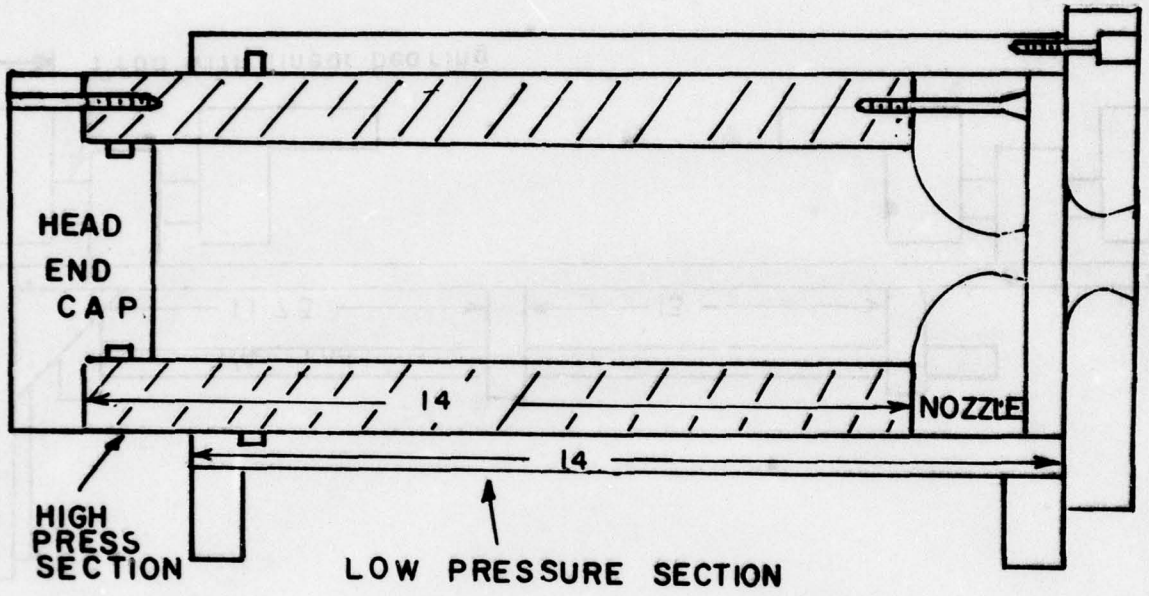

Figure 2. Schematic of Axisymmetric Apparatus.

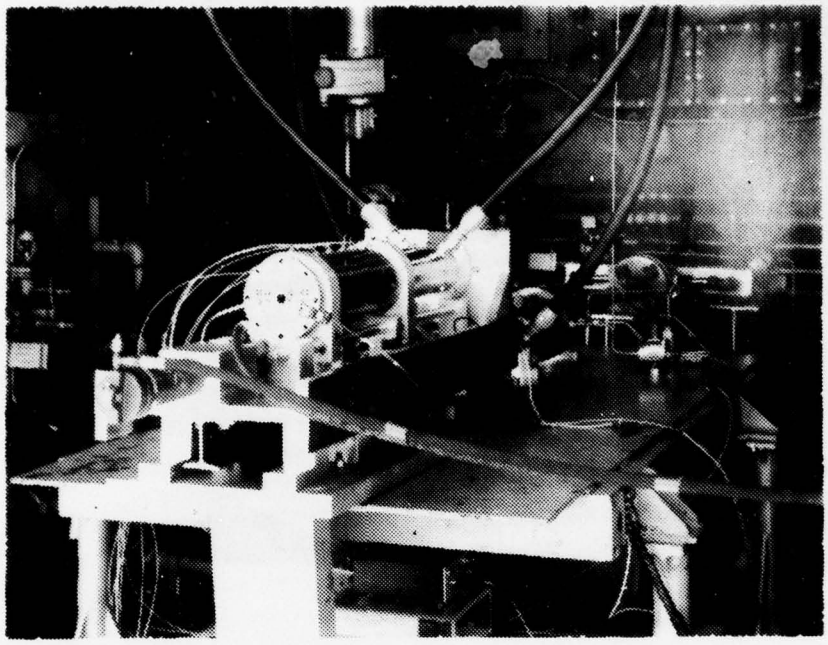

Figure 3. Photograph of Apparatus on Thrust Stand.

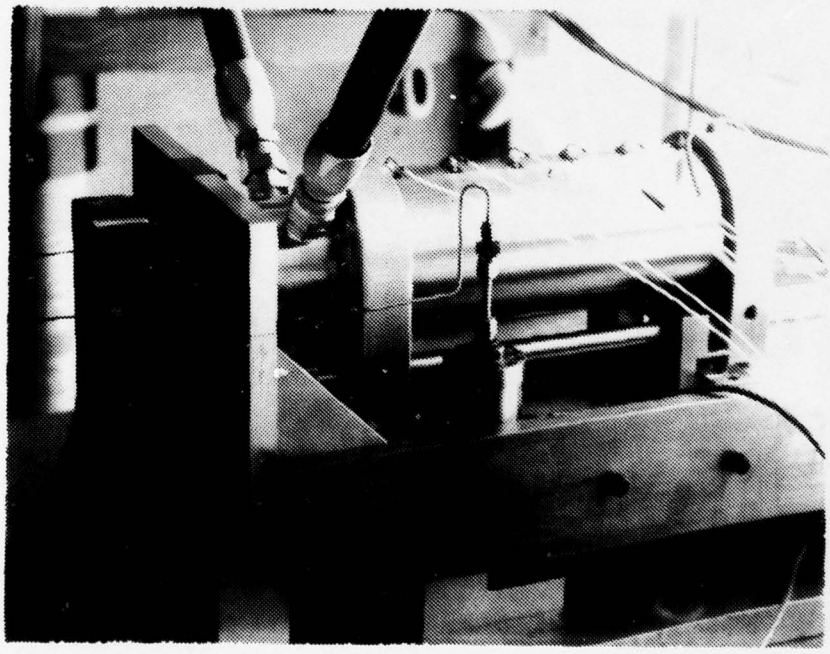

Figure 4. Photograph of Full Forward Position.

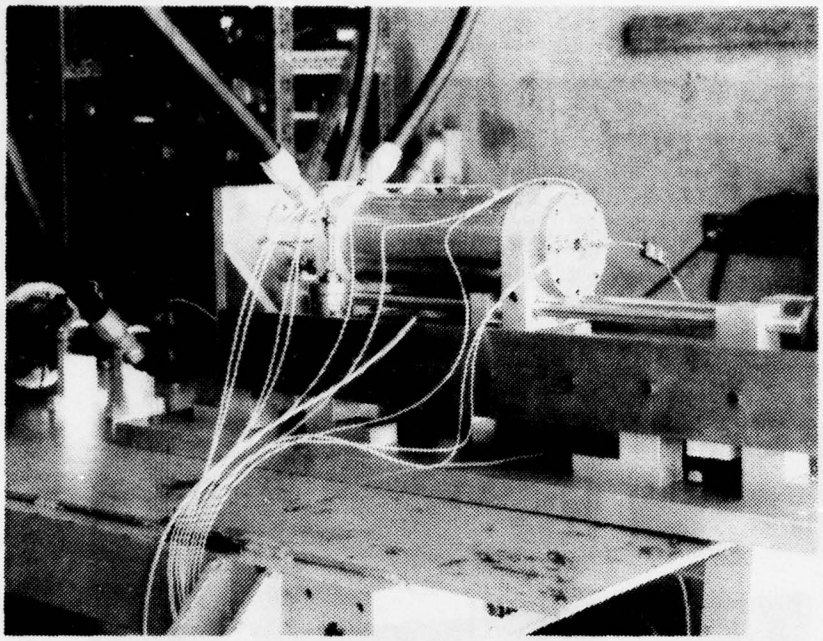

Figure 5. Photograph of Full Forward Position with Instrumentation.

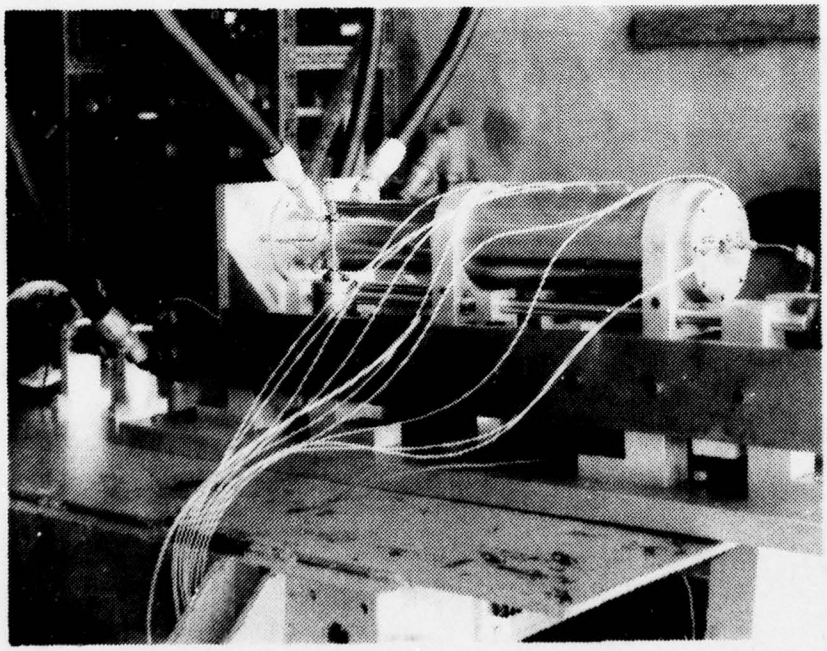

Figure 6. Photograph of Full Aft Position.

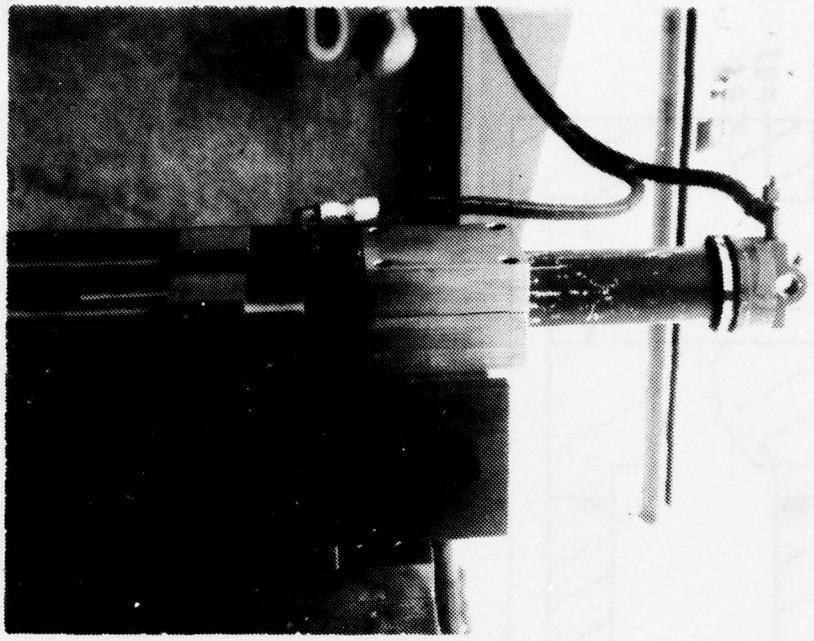

Figure 7. Photograph of Hydraulic Ram.

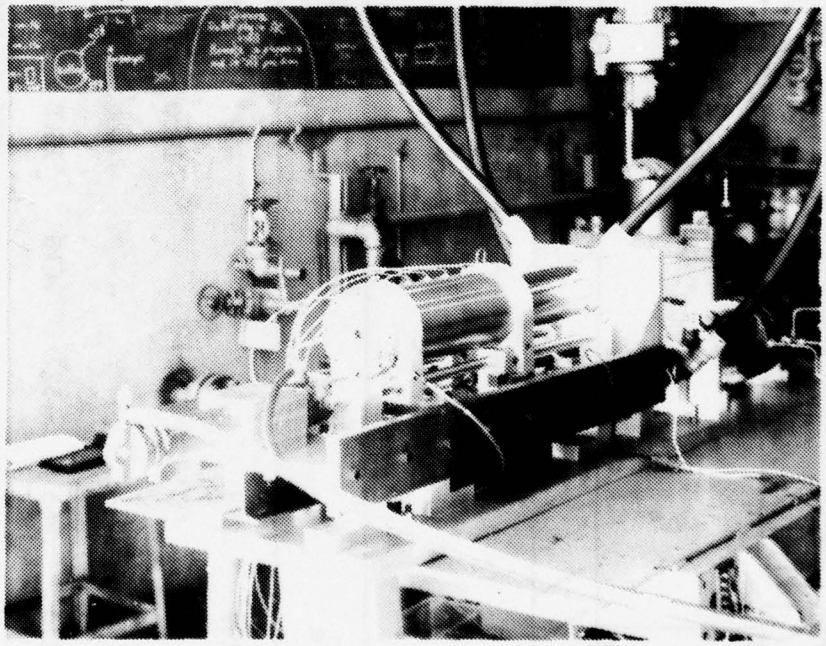

Figure 8. Photograph Showing Thrust Stand Stiffeners.

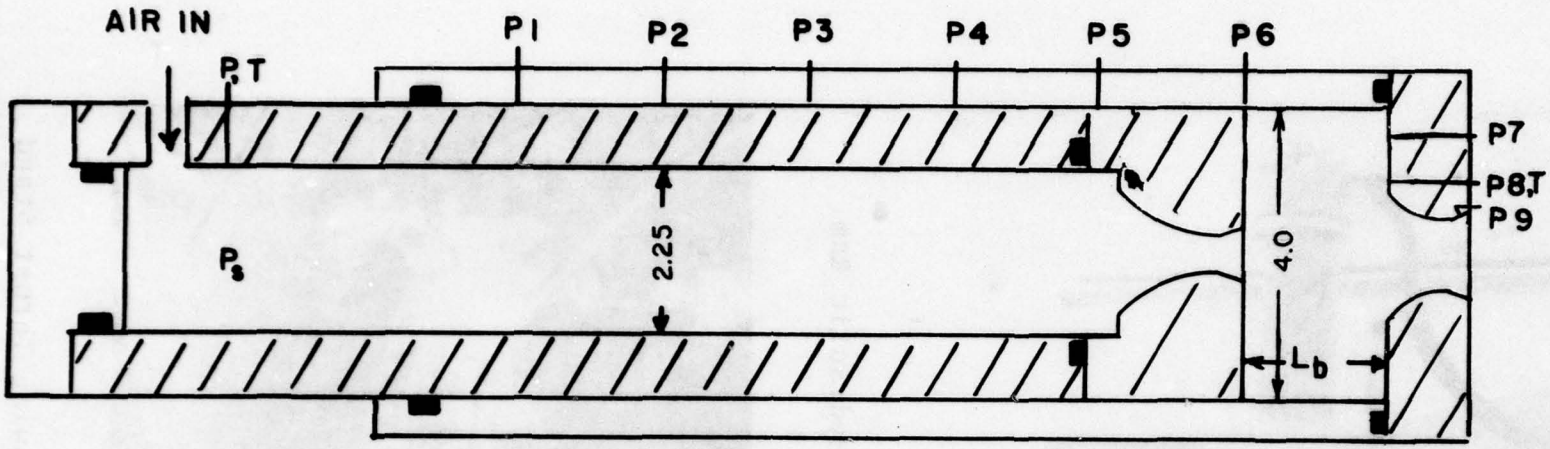

Configuration	d_{t_s}	d_{e_s}	d_{t_b}	d_{e_b}	P_S	P_{SH}	p_{e_s}	p_{e_b}	$A_{t_b/A_{t_s}}$	F_{TH_s}	F_{TH_g}	F_{max}
1 a	.239	.273	.527	.615	1500	308.5	320.7	60.2	4.86	90.7	88.0	104.2
b					1000	205.7	213.8	40.1		60.2	57.2	68.0
c					500	102.8	106.9	20.0		29.7	26.4	31.8
2 a	.273	.465	.527	.615	1500	402.5	76.5	78.5	3.73	130.9	116.2	135.0
b					1000	268.4	51.0	52.3		86.4	76.0	88.6
3 a	.273	.465	1.221	1.330	1500	75.0	76.5	20.0	20.0	130.9	96.6	128.0

Figure 9. Schematic of Apparatus and Test Conditions

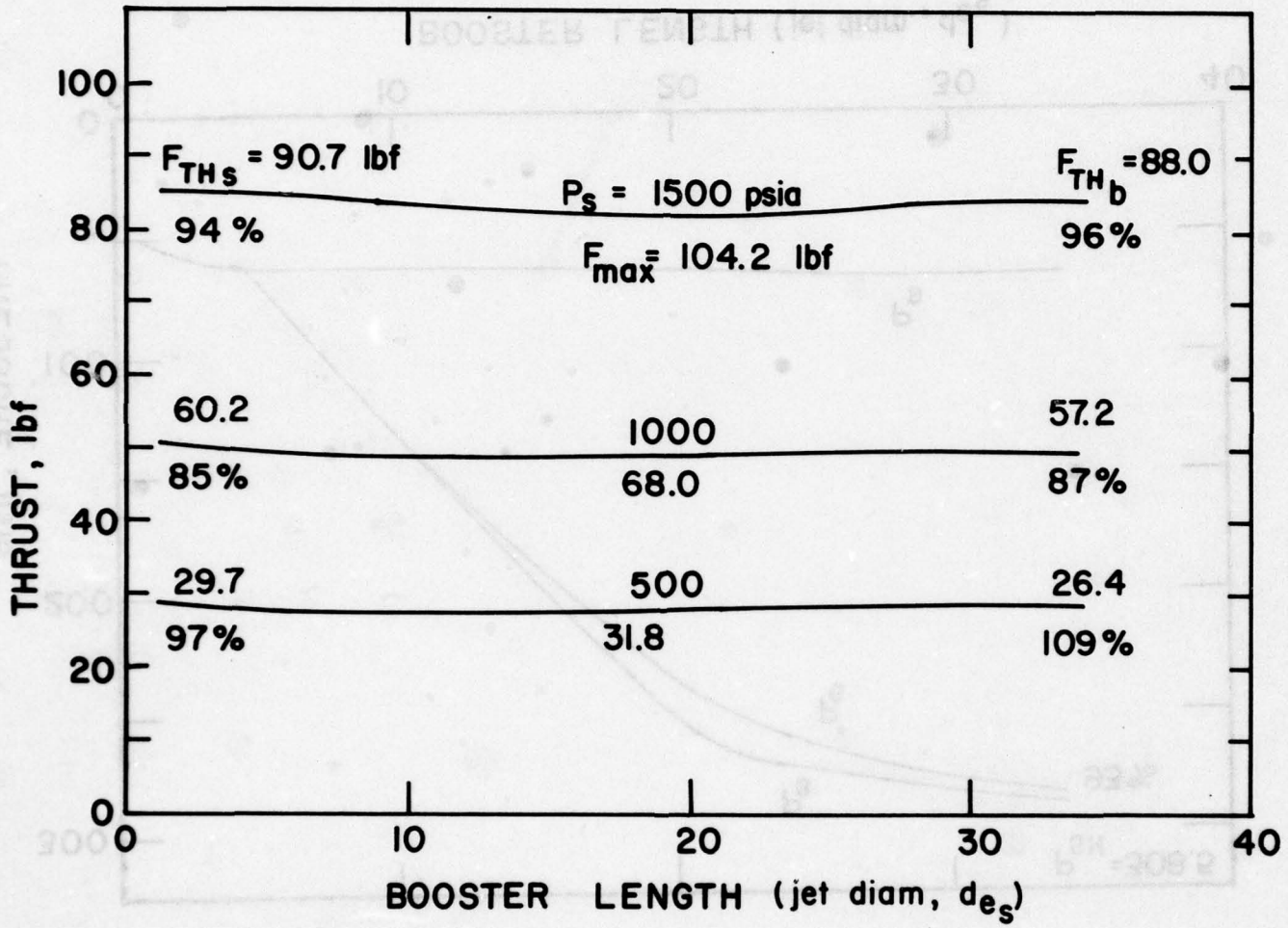

Figure 10. Thrust vs. Booster Cavity Length, Configuration 1, Booster Nozzle on

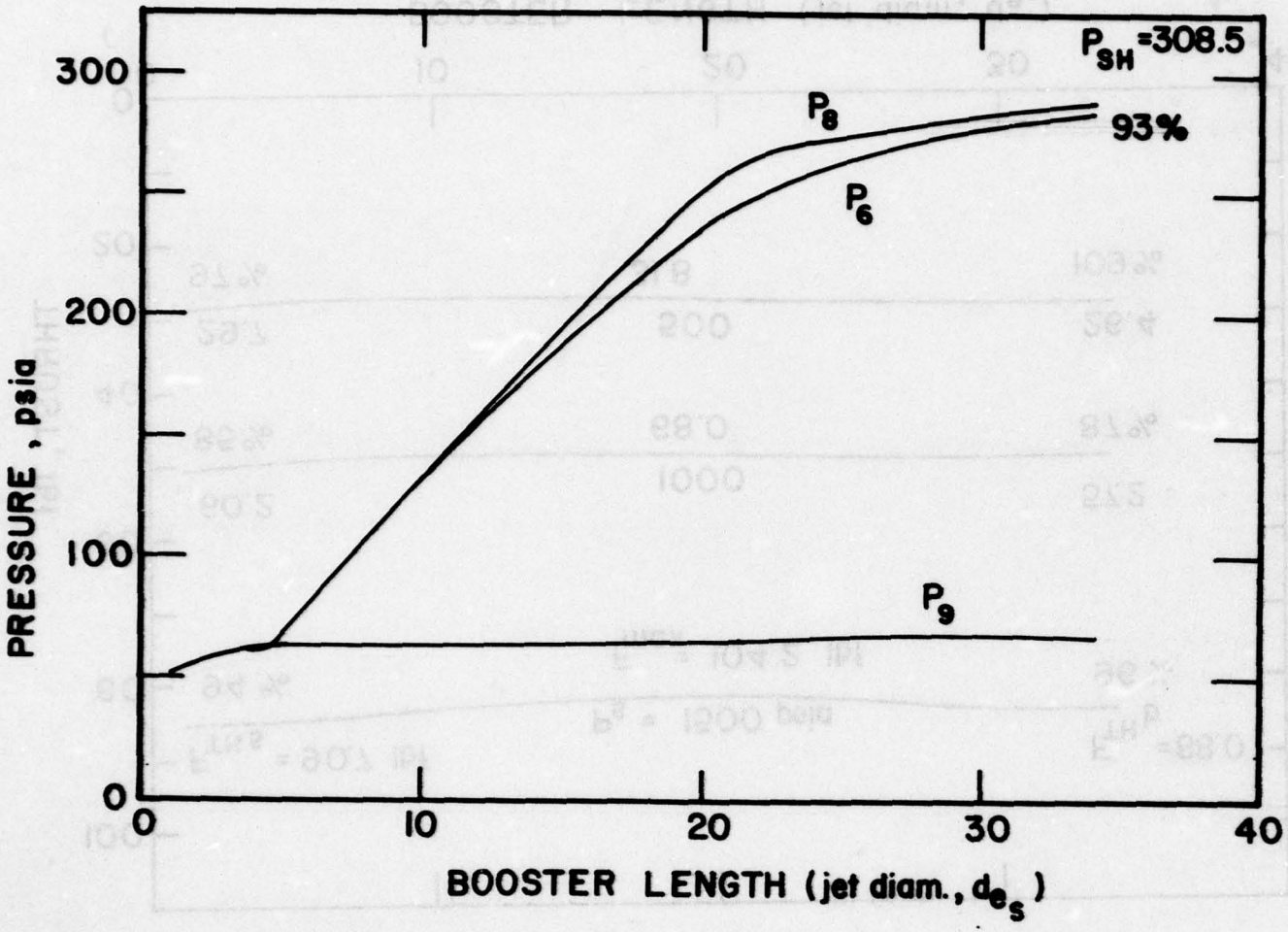

Figure 11. Static Pressures vs. Booster Cavity Length, Configuration 1, P_s = 1500 psia, Booster Nozzle on

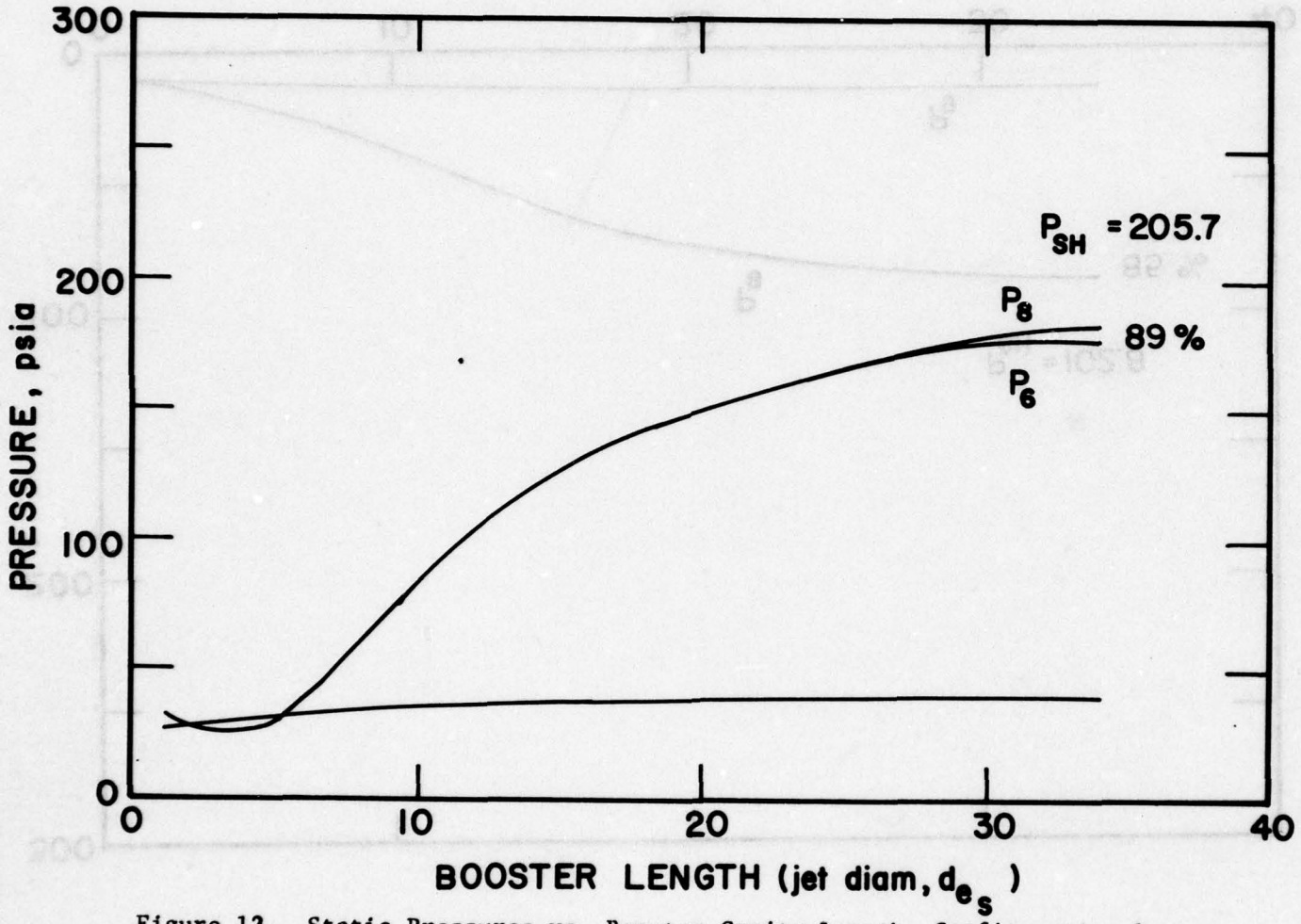

Figure 12. Static Pressures vs. Booster Cavity Length, Configuration 1, P_s = 1000 psia, Booster Nozzle on

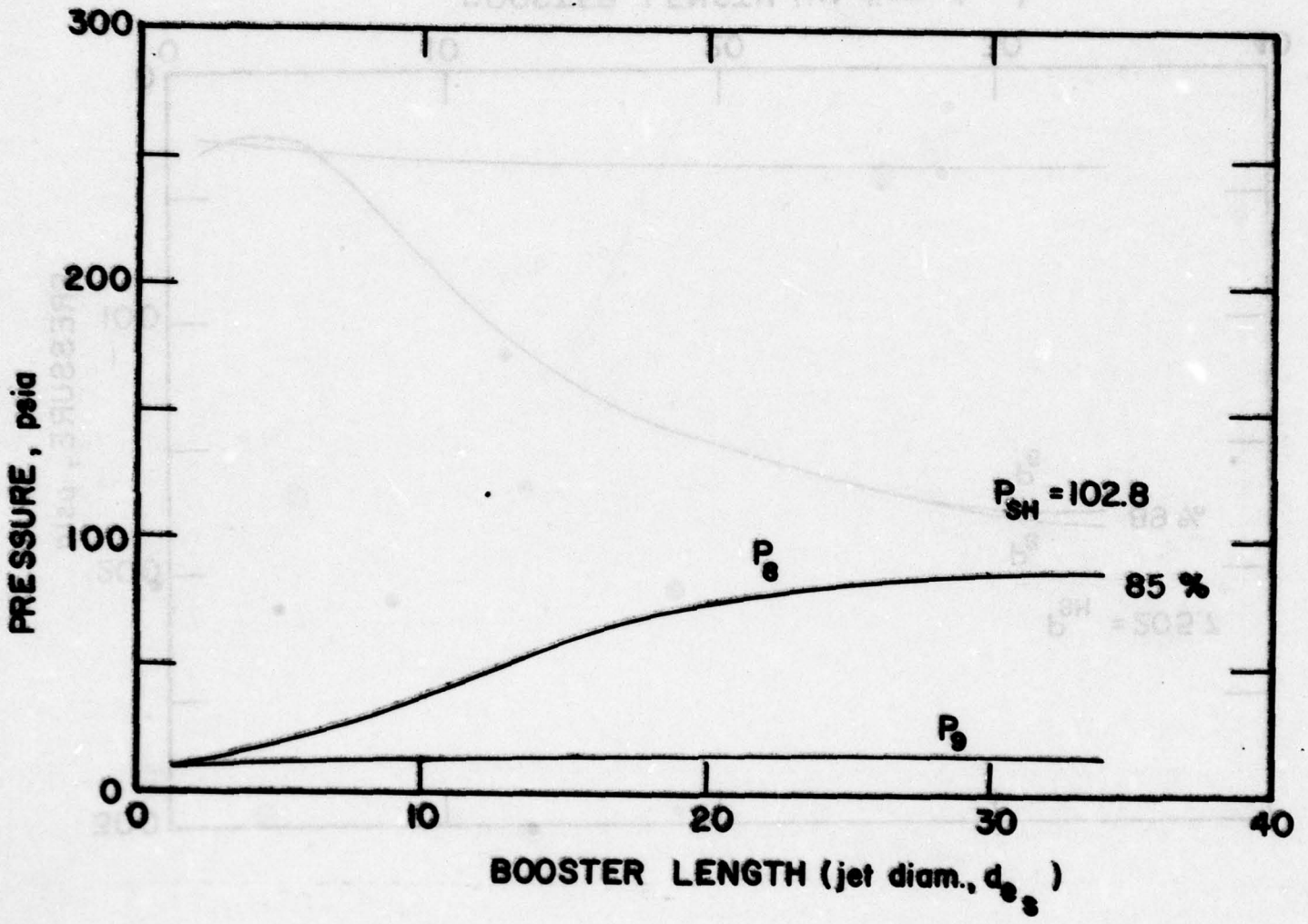

Figure 13. Static Pressures vs. Booster Cavity Length, Configuration 1, P_s = 500 psia, Booster Nozzle on

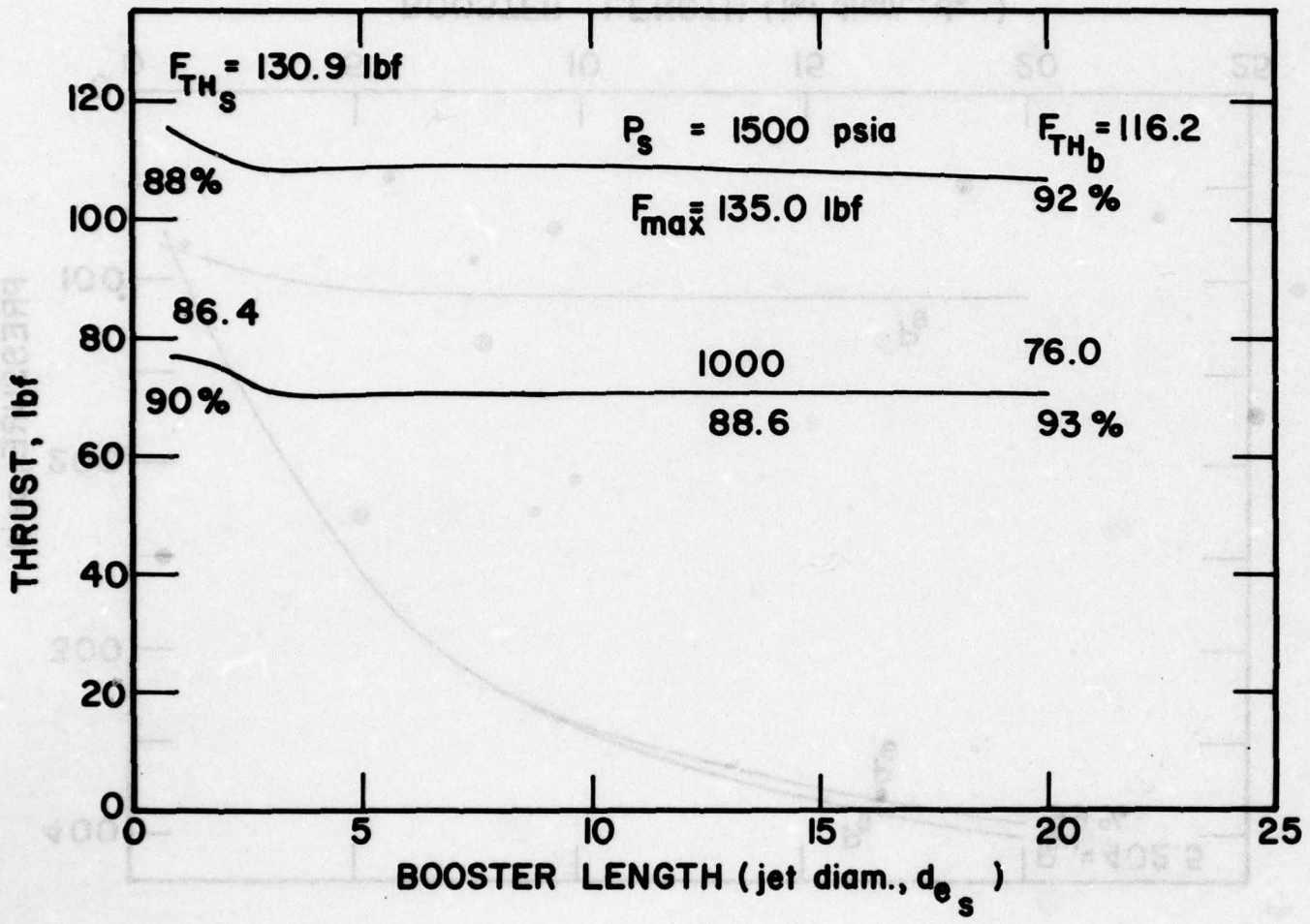

Figure 14. Thrust vs. Booster Cavity Length, Configuration 2, Booster Nozzle on

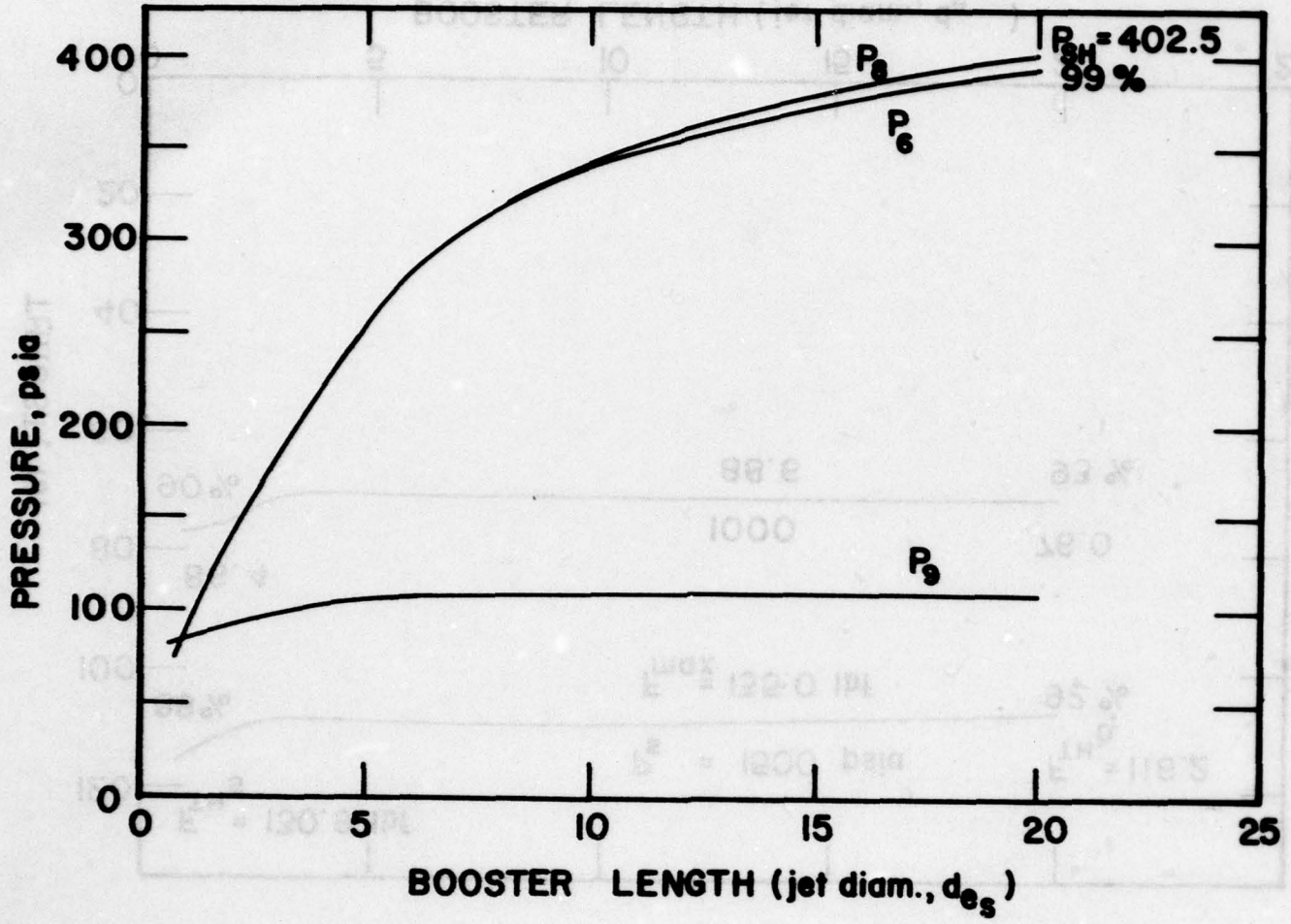

Figure 15. Static Pressures vs. Booster Cavity Length, Configuration 2, P_s = 1500 psia, Booster Nozzle on

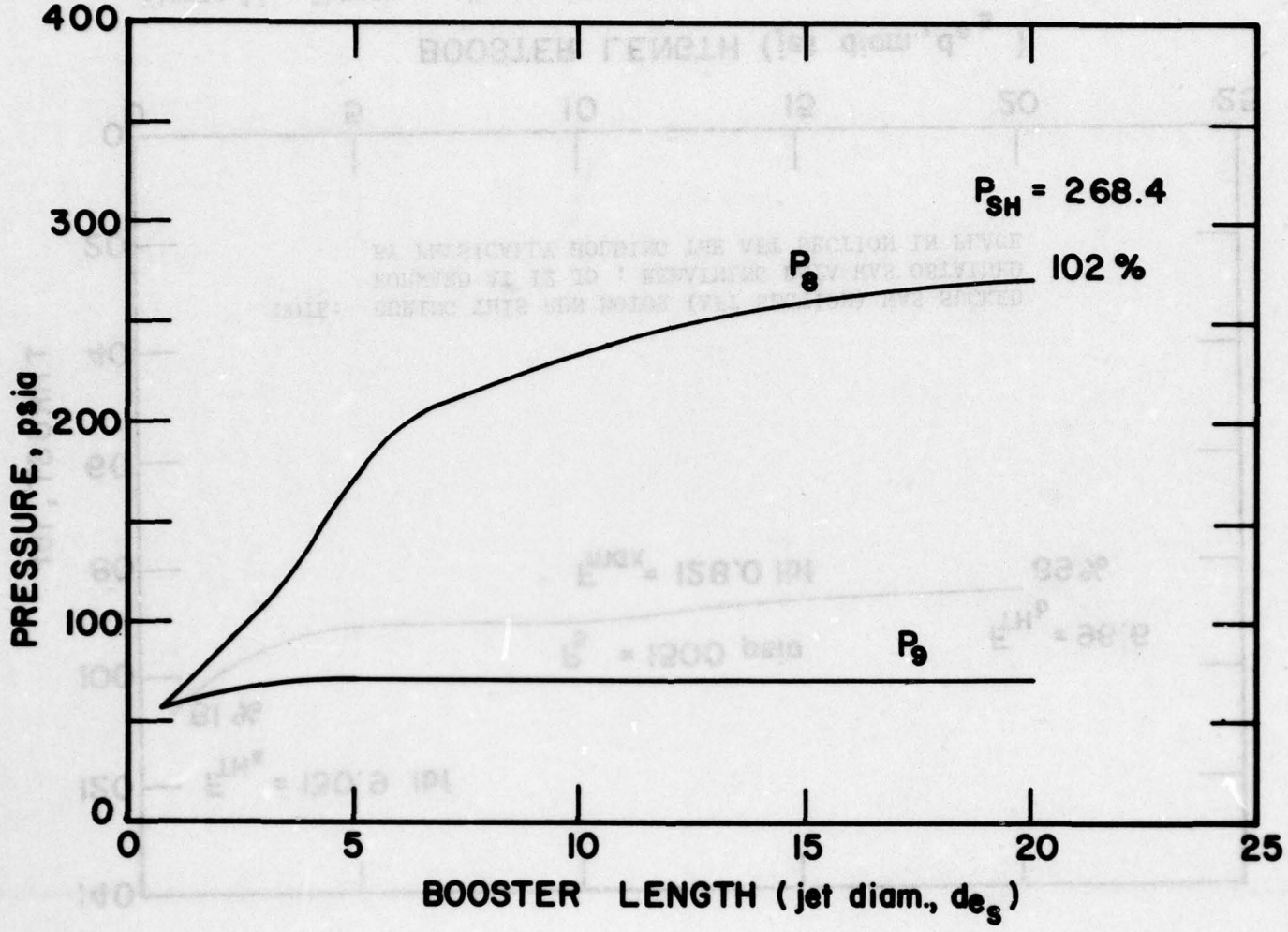

Figure 16. Static Pressures vs. Booster Cavity Length, Configuration 2, P_s = 1000 psia, Booster Nozzle on

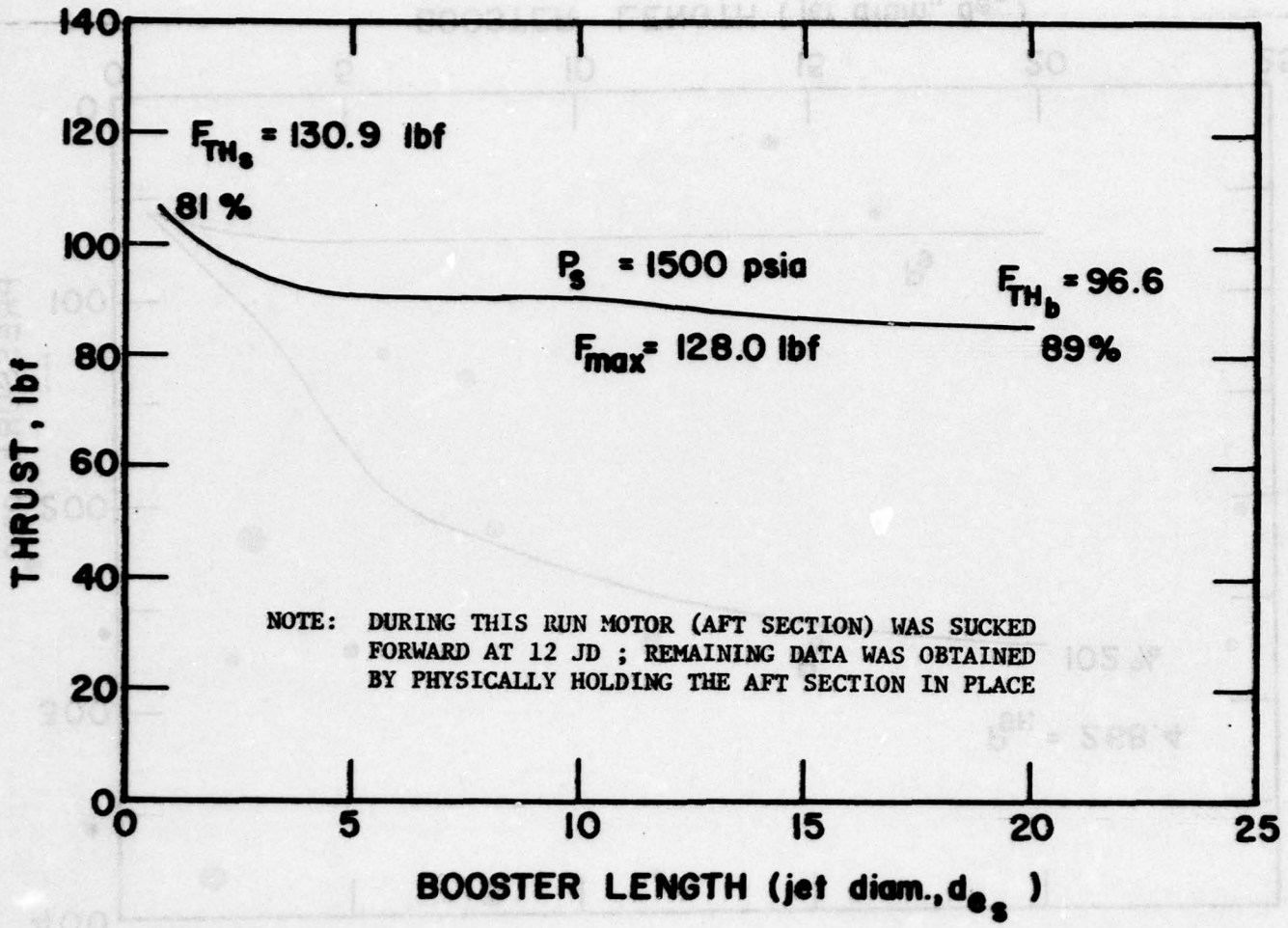

Figure 17. Thrust vs. Booster Cavity Length, Configuration 3, Booster Nozzle on

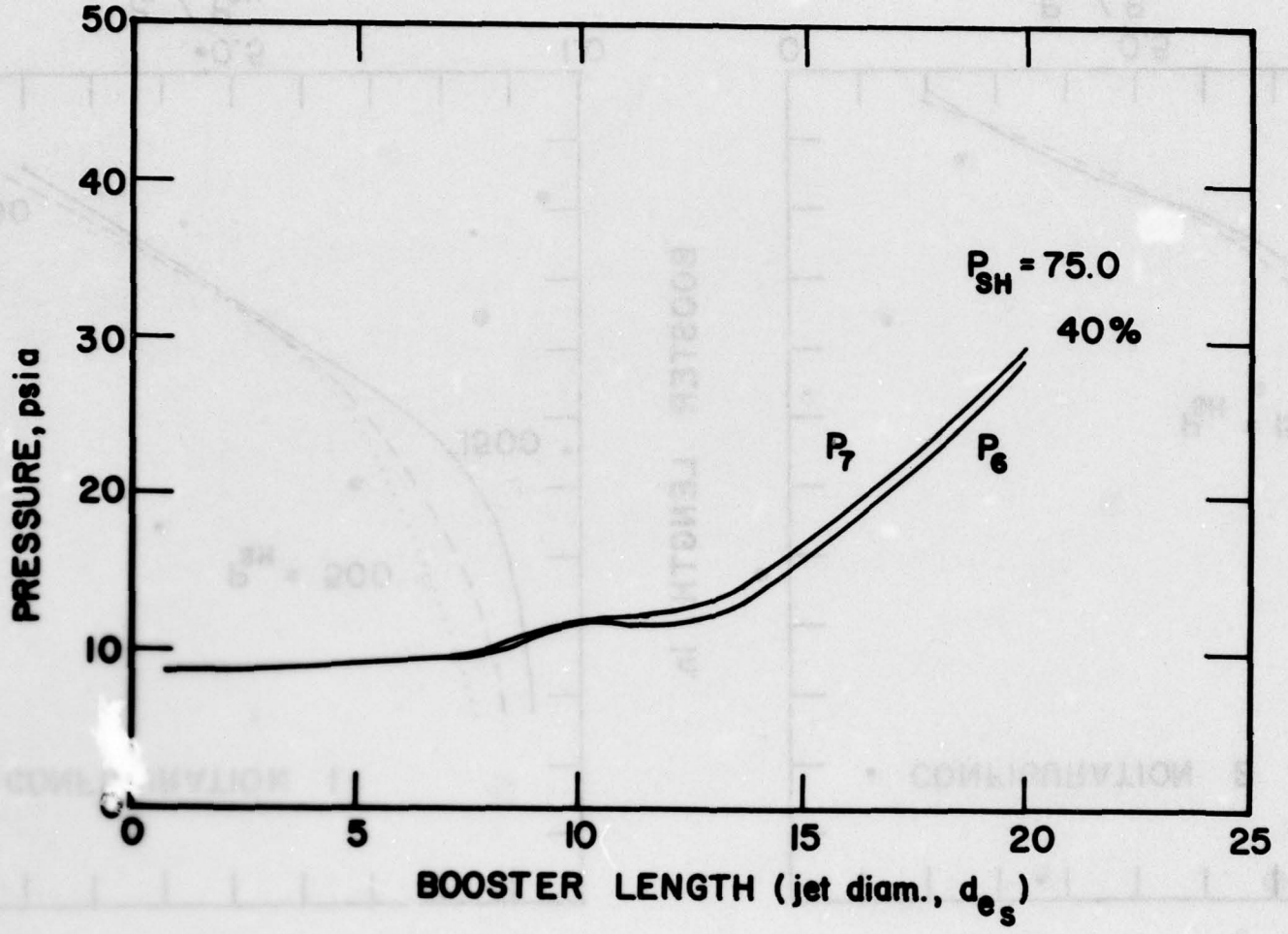

Figure 18. Static Pressure vs. Booster Cavity Length, Configuration 3, P_s = 1500 psia, Booster Nozzle on

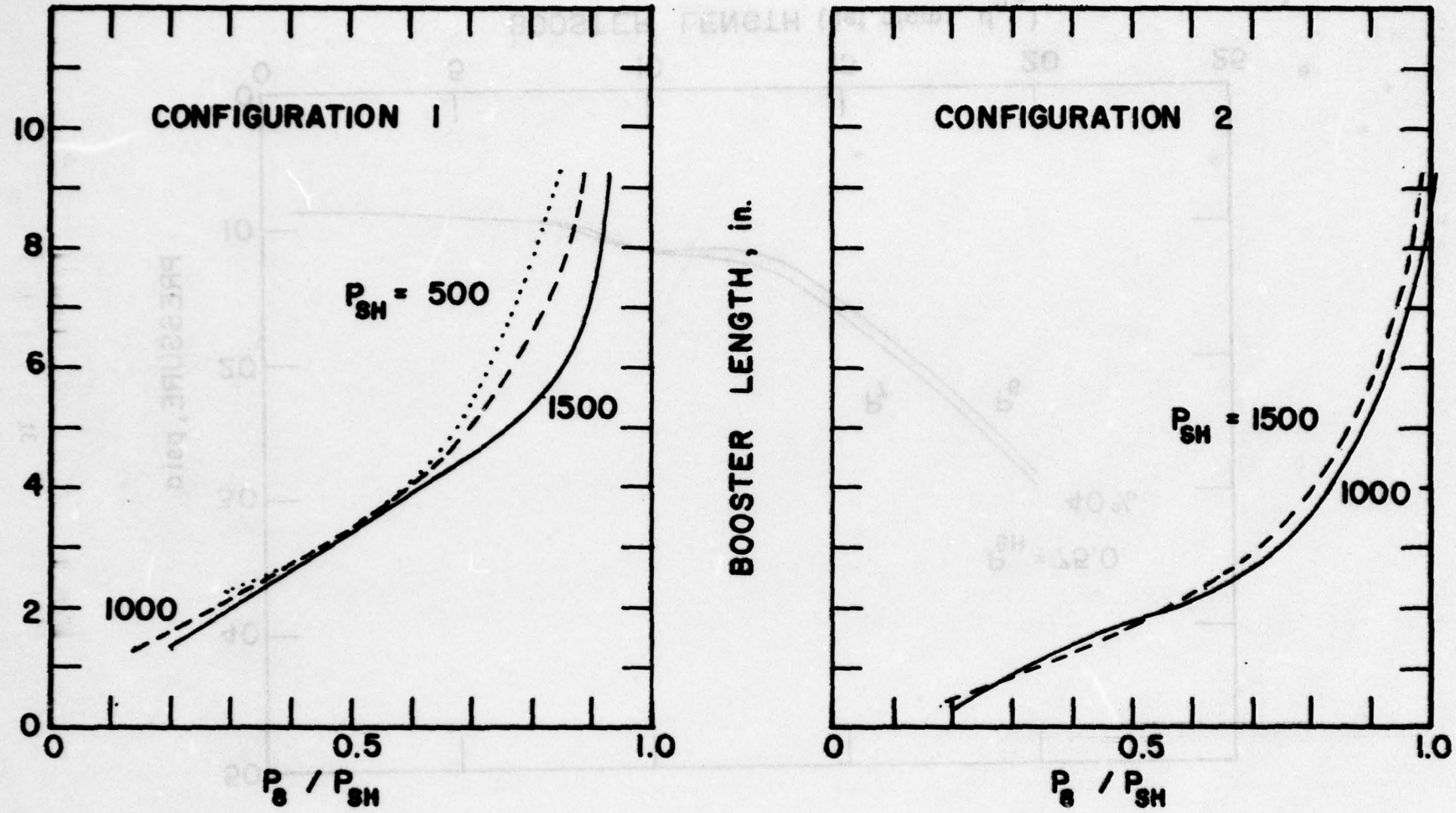

Figure 19. Fraction of Shockdown Pressure vs. Booster Cavity Length

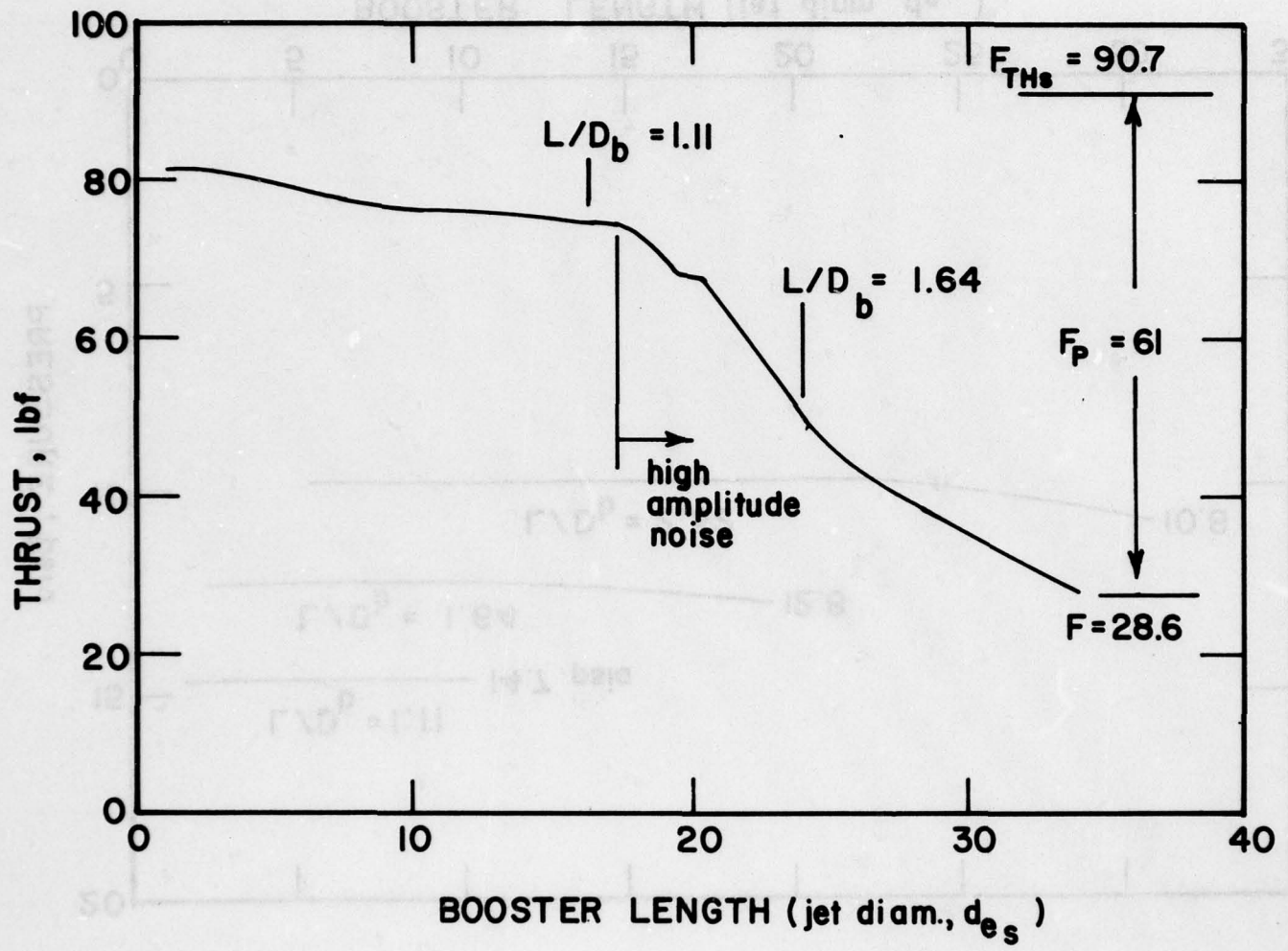

Figure 20. Thrust vs. Booster Cavity Length, Configuration 1, P_s = 1500 psia, Booster Nozzle off

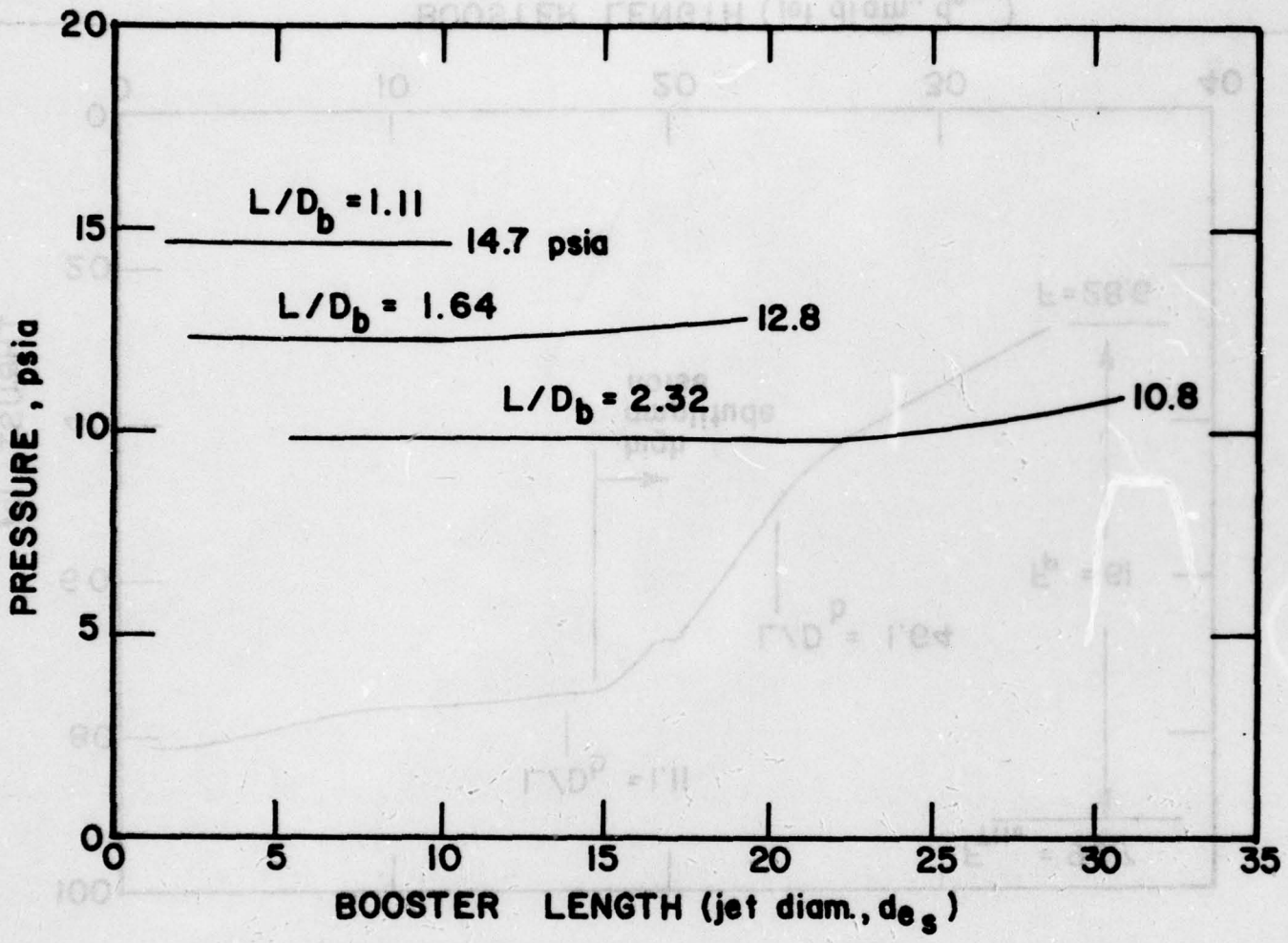

Figure 21. Static Pressure vs. Booster Cavity Length, Configuration 1, P_s = 1500 psia, Booster Nozzle off

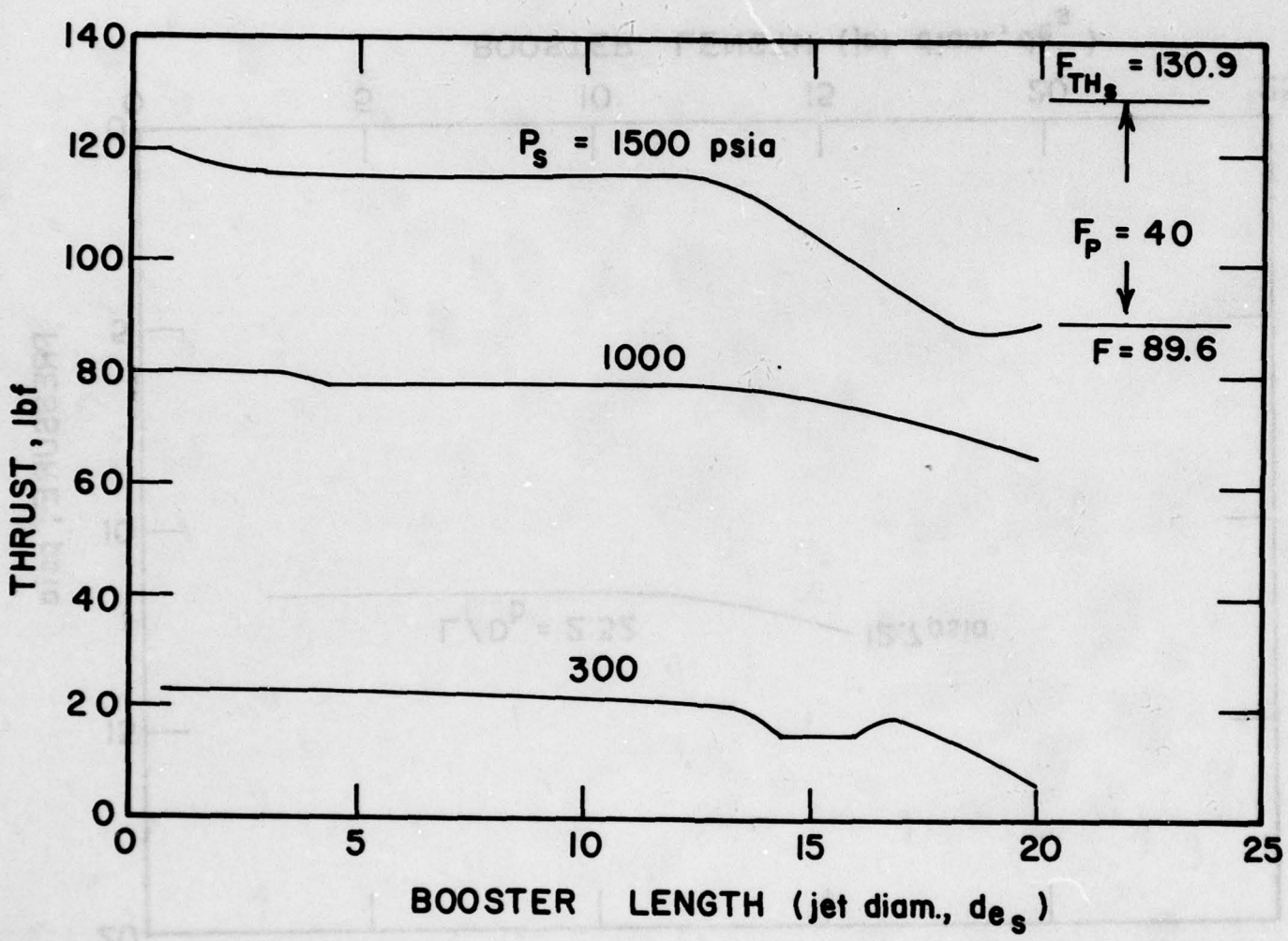

Figure 22. Thrust vs. Booster Cavity Length, Configuration 2, Booster Nozzle off

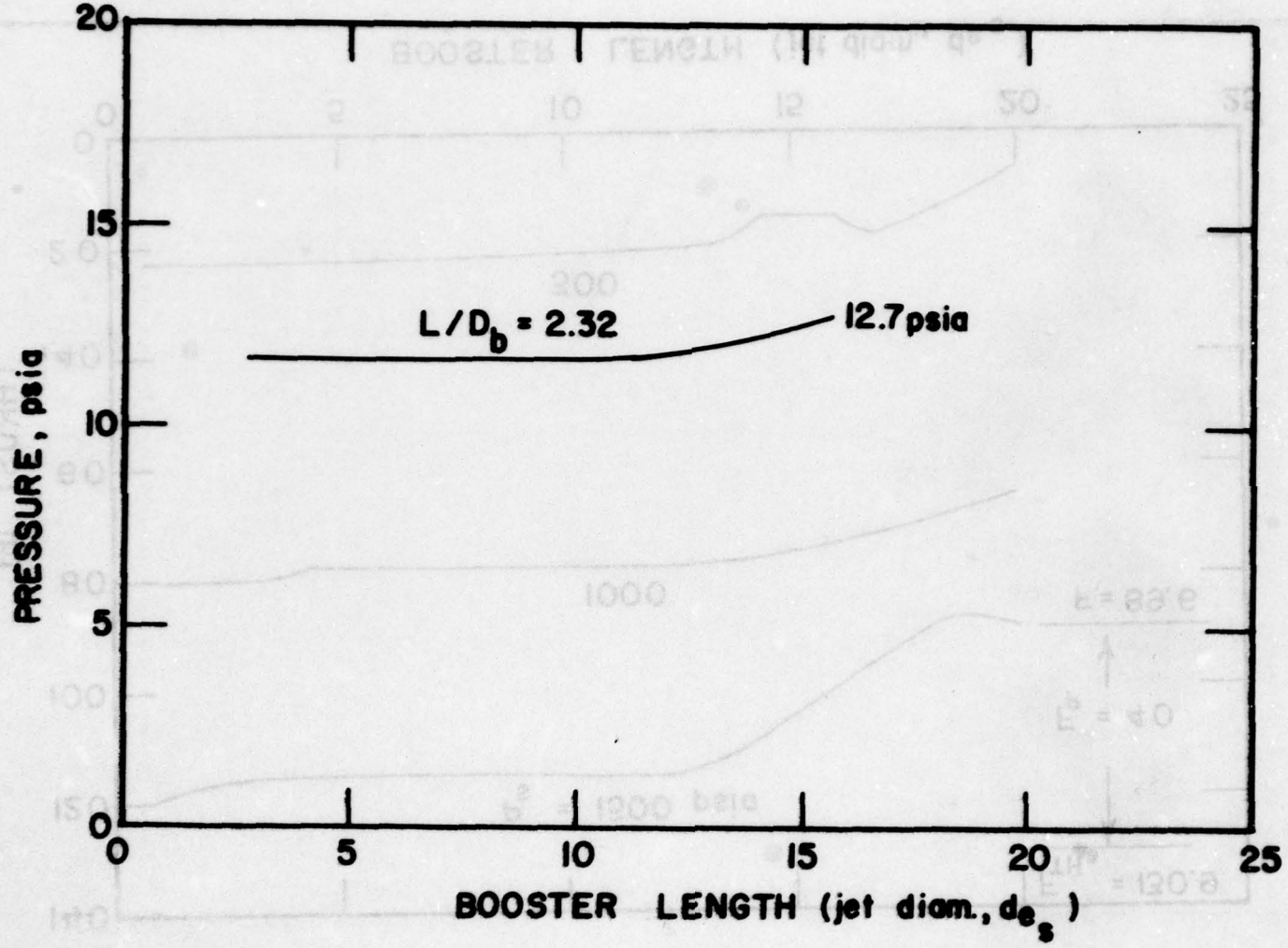

Figure 23. Static Pressure vs. Booster Cavity Length, Configuration 2, P_s = 1500 psia, Booster Nozzle off

LIST OF REFERENCES

1. Donaldson, C. and Gray, K., "Theoretical and Experimental Investigation of the Compressible Free Mixing of Two Dissimilar Gases," AIAA J., Vol. 4, No. 11, pp. 2017-2025, November 1966.

2. Tufts, L. W. and Smoot, L. D., "A Turbulent Mixing Coefficient Correlation for Coaxial Jets with and without Secondary Flows," J. of Spacecraft and Rockets, Vol. 8, No. 12, pp. 1183-1190, December 1971.

3. Morris, P. J., "Turbulence Measurements in Subsonic and Supersonic Axisymmetric Jets in Parallel Stream," AIAA J., Vol. 14, No. 10, pp. 1468-1475, October 1976.

4. Benham, C. B. and Wirtz, D. P., "Dual-Chamber Performance Analysis," NWC Memorandum to J. Andrews 3245/CBB: CAS, Reg. 3245-40-77, 5 May 1977.

5. Zucrow, M. J. and Hoffman, J. D., Gas Dynamics, Vol. I, John Wiley and Sons, 1976, pp. 394-401.

6. Gawain, T. H., "A Mathematical Model for Turbulent Flows Involving Supersonic Subsonic, and Recirculating Regions", Naval Postgraduate School Report NPS67Gn78003, July 1978.

DISTRIBUTION LIST

		No. of Copies
1.	Library Code 0142 Naval Postgraduate School Monterey, CA 93940	2
2.	Department of Aeronautics Code 67 Naval Postgraduate School Monterey, CA 93940	
	M. F. Platzer, Chairman	1
	D. W. Netzer	12
	T. H. Gawain	2
3.	Dean of Research Code 012 Naval Postgraduate School Monterey, CA 93940	1
4.	Defense Documentation Center Cameron Station Alexandria, VA 22314	2
5.	Commanding Officer Naval Air Systems Command Department of the Navy Washington, DC 20360 (AIR-03B, 03P2, 30212, 320, 340B, 503, 510B, 5105, 5203C, 5312, 532, 5366)	13
6.	Chief of Naval Material Department of the Navy Washington, DC 20360 (MAT-030B, 032, NSP-27, 2731)	4
7.	Commanding Officer Naval Sea Systems Command Headquarters Washington, DC 20362 (Attn: Code 6542D)	1
8.	Commanding General Marine Corps Development and Education Command Quantico, VA 22134 (Attn: Director, Marine Corps Landing Force Development Center)	3

No. of Copies

9. Commander — 1
Air Test & Evaluation Squadron
5-VX-5
Naval Air Facility
China Lake, CA 93555

10. Officer in Charge — 1
Fleet Analysis Center
Naval Weapon Station, Seal B
Corona, CA 91720

11. Commanding Officer — 1
Naval Ammunition Depot
Hawthorne, NV 89415
(Code 05, Robert Dempsey)

12. Commanding Officer — 1
Naval Explosive Ordnance Disposal
Facility
Indian Head, MD 20640

13. Commanding Officer — 1
Naval Intelligence Support Center
4301 Suitland Road
Washington, DC 20390
(Attn: 00XA, CDR Jack Darnell)

14. Commanding Officer — 1
Naval Ocean Systems Center
San Diego, CA 92152
(Attn: Code 133)

15. Commanding Officer — 1
Naval Ordnance Station
Indian Head, MD 20640
(Attn: Code PM)

16. Naval Surface Weapons Center — 2
Dahlgren Laboratory
Dahlgren, VA 22448
(Code DG, Attn: C. L. Dettinger)

17. Commanding Officer — 1
Naval Surface Weapons Center
White Oak
Silver Spring, MD 20910
(Attn: Code WR)

No. of Copies

18. Commanding Officer — 1
Naval Intelligence Support Center
Liaison Officer
4301 Suitland Road
Washington, DC 20390
(Attn: LNN)

19. Commanding Officer — 1
Army Armament Materiel Readiness Command
Rock Island, IL 61201
(Attn: DRSAR-LEM)

20. Commanding General — 4
Army Ballistic Research & Development Center
Dover, NJ 07801
(Attn: SMD, Concepts Branch)

21. Commanding Officer — 1
Army Ballistic Research Laboratories
Aberdeen Proving Ground, MD 21005
(Attn: DRDAR-TSB-S (STINFO)

22. Headquarters — 2
Air Force Systems Command
Andrews Air Force Base
Washington, DC 20334
(Attn: DLFP, SDW)

23. Commanding Officer — 2
Air Force Armament Laboratory
Eglin Air Force Base, FL 32542
(Attn: DLJW, DLR)

24. Commanding Officer — 1
Air Force Rocket Propulsion Lab.
Edwards AFB, CA 93523
(Attn: MKP)

25. Commanding Officer — 2
Foreign Technology Division
Wright-Patterson AFB, OH 45433
(Attn: Code PDXA, James Woodard,
Code XRHP)

26. Defense Advanced Research Projects Agency — 1
1400 Wilson Blvd.
Arlington, VA 22209

No. of Copies

27. Chairman — 1
Department of Defense Explosives Safety Board
Room 856-C, Hoffman Bldg. 1
2461 Eisenhower Avenue
Alexandria, VA 22331
(Attn: 6-A-145)

28. George C. Marshall Space Flight Center — 1
Huntsville, AL 35812
(Attn: S&E-ASTN-PJ, Ken Reed)

29. Naval Weapon Center — 37
China Lake, CA 93555
(Attn: Code 3205)